FLUTTER OF DARRIEUS WIND TURBINE BLADES

Norman D. Ham
Department of Aeronautics and Astronautics
Massachusetts Institute of Technology
Cambridge, Mass. 02139

ABSTRACT

The testing of Darrieus wind turbines has indicated that under certain conditions, serious vibrations of the blades can occur, involving flatwise bending, torsion, and chordwise bending. It is the purpose of this paper to develop a theoretical method of predicting the aeroelastic stability of the coupled bending and torsional motion of such blades with a view to determining the cause of these vibrations and a means of suppressing them.

1. Introduction

The troposkien type of vertical-axis wind turbine, Reference 1, embodies flexible curved blades connected at each end to the top and bottom of a vertical shaft which permits the blades to rotate about the vertical axis under the action of the wind. The curve of each blade is ideally that of a troposkien; i.e., the shape taken by a flexible cable of uniform density and cross section whose ends are attached to two points on a vertical axis, when it is spun at a constant angular velocity about the vertical axis. In this manner the bending stresses in the blades are eliminated.

The testing of such devices has indicated that under certain conditions, serious vibrations of the blades can occur, involving flatwise bending, torsion, and chordwise bending. It is the purpose of this report to develop a theoretical method of predicting the aeroelastic stability of the coupled bending and torsional motion of such blades with a view to determining the cause of these vibrations and a means of suppressing them. The present analysis is an extension of that of Reference 2.

2. Flatwise Bending Vibration of the Ideal Troposkien

Consider the rotating troposkien-type rotor blade shown in Figure 1. The bending moment at x is given by

$$M(x) = \int_0^x \{[y_o+y(\xi)]\Omega^2 - \ddot{y}(\xi)\}\, m(\xi)\, (x-\xi)\, d\xi - H[y(o) - y(x)]$$

where

Ω = rotor rotational speed

$m(\xi)$ = rotor blade mass at ξ per unit of x-distance

H = blade tension force at mid-point between blade ends

Differentiating the bending moment equation twice with respect to x,

$$\frac{\partial^2 M(x)}{\partial x^2} = [y_o+y(x)]\, \Omega^2 m(x) - \ddot{y}(x)\, m(x) + H \frac{\partial^2 y}{\partial x^2}$$

This work was sponsored by Sandia Laboratories, Albuquerque, New Mexico, for the U.S. Energy Research and Development Administration.

From the theory of elasticity for the bending of slender beams,

$$M(x) = EI \frac{\partial^2 y}{\partial x^2}$$

Therefore

$$\frac{\partial^2 M(x)}{\partial x^2} = \frac{\partial^2}{\partial x^2} \left[EI \frac{\partial^2 y}{\partial x^2}\right]$$

Then the blade bending equation of motion is

$$\frac{\partial^2}{\partial x^2} \left[EI \frac{\partial^2 y}{\partial x^2}\right] - H \frac{\partial^2 y}{\partial x^2} - \Omega^2 m(x) \ (y_o+y) + m(x)\ddot{y} = 0 \qquad (1)$$

Note that $m(x)\,dx = m(s)\,ds$, where s = arc length along the blade, and $m(s) = m$, a constant. Then

$$m(x) = m \frac{ds}{dx} = m \left[1 + \left(\frac{dy}{dx}\right)^2\right]^{1/2}$$

Equation (1) is the equation of the vibrating blade: the steady-state case is described and solved in Reference 1. For present purposes, consider the equation which results when it is assumed that $y = y(\theta)$:

$$\frac{\partial^2}{\partial \theta^2} \left[EI \frac{\partial^2 y}{\partial \theta^2} \left(\frac{\partial \theta}{\partial x}\right)^2\right] \left(\frac{\partial \theta}{\partial x}\right)^2 - H \frac{\partial^2 y}{\partial \theta^2} \left(\frac{\partial \theta}{\partial x}\right)^2 - \Omega^2 m(\theta) \ [y_o+y(\theta)] + m(\theta)\ddot{y}(\theta) = 0 \qquad (2)$$

Let $y = \sum_{n=1}^{\infty} y_n(\theta)\ g_n(t)$

Substituting into Equation (2), there results

$$\frac{\partial^2}{\partial \theta^2} \left[EI \sum_{n=1}^{\infty} \frac{\partial^2 y_n}{\partial \theta^2} \left(\frac{\partial \theta}{\partial x}\right)^2 g_n\right] \left(\frac{\partial \theta}{\partial x}\right)^2$$

$$-H \sum_{n=1}^{\infty} \frac{\partial^2 y_n}{\partial \theta^2} \left(\frac{\partial \theta}{\partial x}\right)^2 g_n - \Omega^2 m \left[y_o + \sum_{n=1}^{\infty} y_n\ g_n\right] + m \sum_{n=1}^{\infty} y_n\ \ddot{g}_n = 0 \qquad (3)$$

Assume free vibration of the blade in the nth flatwise mode in a vacuum:

$$g_n = \bar{g}_n e^{i\omega_n t}$$

$$\ddot{g}_n = -\omega_n^2 \bar{g}_n e^{i\omega_n t} = -\omega_n^2 g_n$$

Substituting into the nth term of Equation (3), i.e., the equation for free vibrations in the nth mode,

$$\frac{\partial^2}{\partial\theta^2}\left[EI \frac{\partial^2 y_n}{\partial\theta^2} \left(\frac{\partial\theta}{\partial x}\right)^2 g_n\right] \left(\frac{\partial\theta}{\partial x}\right)^2 - H \frac{\partial^2 y_n}{\partial\theta^2} \left(\frac{\partial\theta}{\partial x}\right)^2 g_n - \Omega^2 m \left[y_o + y_n g_n\right] = m \omega_n^2 y_n g_n \tag{4}$$

Then including all modes, substitute Equation (4) into Equation (3) to obtain

$$m \sum_{n=1}^{\infty} y_n \ddot{g}_n + m \sum_{n=1}^{\infty} \omega_n^2 y_n g_n = 0 \tag{5}$$

This is the equation for flatwise free vibration in a vacuum of the rotating ideal troposkien blade.

3. Flatwise Bending Vibration of the Approximate Troposkien

Reference 3 describes an approximation to the troposkien shape consisting of straight and circular-arc segments. In this instance, the origin of the axis system shown in Figure 1 is located at the center of the circular-arc segment, and the distance y_o of the origin to the axis of rotation is determined by the geometry of the straight segments.

Reference 4 suggests the following approximate mode shapes for the flatwise vibration of non-rotating circular arcs of radius R with pinned ends:

$$y_n = R \sin\left(\frac{n\pi}{\alpha}\right)\theta \tag{6}$$

This expression was shown in Reference 2 to be an approximate solution to the eigenvalue equation describing the vibration of rotating circular arcs, for the case $\alpha = \pi$ and $y_o = 0$.

The vibration frequencies are given by the expression

$$\omega_n^2 = \omega_{n_o}^2 + K_n \Omega^2 \tag{7}$$

where ω_{n_o} and K_n must be determined experimentally, or numerically by finite-element analysis. For the special case of Reference 2, $K_n = n^2 - 1$.

Then Equations (5), (6), (7) describe approximately the flatwise free bending vibration in a vacuum of the circular-arc segment of the rotating approximate troposkien blade.

4. Torsion/Chordwise Bending Vibration of the Approximate Troposkien

Reference 5 considers the torsion/chordwise bending vibration of non-rotating circular arcs. The forces due to rotation are shown in Figure 2. Adding these forces to the equations of Reference 5, in the nomenclature of the present analysis the torsion/chordwise bending equations become, for the circular-arc segment of the approximate troposkien blade,

$$z'^{v} - R\beta'' - k\,(z'' + R\beta'') = \frac{mR^4}{EI_2}\left(\ddot{z} - z\Omega^2 - 2\Omega\dot{y} - \frac{H}{mR^2}\,z''\right) \tag{8}$$

$$z'' - R\beta + k(R\beta'' + z'') = 0 \tag{9}$$

where $\beta(\theta)$ = blade torsional displacement

$z(\theta)$ = blade chordwise bending displacement

R = radius of circular arc

k = GK/EI_2

GK = torsional stiffness of blade section

EI_2 = chordwise bending stiffness of blade section

m = rotor blade mass per unit length of blade

Note that flatwise and torsion/chordwise bending are coupled dynamically only by the Coriolis forces $2\Omega ym$ and $2\Omega\dot{z}m$.

Let $z = \sum_{n=1}^{\infty} z_n(\theta)\ f_n(t)$

$\beta = \sum_{n=1}^{\infty} \beta_n(\theta)\ f_n(t)$

Substituting into Equation (8), and neglecting the Coriolis coupling term at present, there results

$$\sum_{n=1}^{\infty} z_n^{IV} f_n - R \sum_{n=1}^{\infty} \beta_n'' f_n - k \left(\sum_{n=1}^{\infty} z_n'' f_n + R \sum_{n=1}^{\infty} \beta_n'' f_n \right)$$

$$= \frac{mR^4}{EI_2} \left(\sum_{n=1}^{\infty} z_n \ddot{f}_n - \Omega^2 \sum_{n=1}^{\infty} z_n f_n - \frac{H}{mR^2} \sum_{n=1}^{\infty} z_n'' f_n \right) \qquad (10)$$

Assume free vibration of the blade in the nth torsion/chordwise bending mode in a vacuum:

$$f_n = \bar{f}_n\ e^{i\bar{\omega}_n t}$$

$$\ddot{f}_n = -\omega_n^2\ \bar{f}_n\ e^{i\bar{\omega}_n t} = -\bar{\omega}_n^2\ f_n$$

Substituting into the nth term of Equation (10), i.e., the equation for free vibrations in the nth mode,

$$\frac{EI_2}{mR^4} \cdot [z_n^{IV} f_n - R\beta_n'' f_n - k(z_n'' f_n + R\beta_n'' f_n)] + \Omega^2 m\ z_n f_n + \frac{H}{R^2} z_n'' f_n$$

$$= -m\ z_n\ \omega_n^2\ f_n \qquad (11)$$

Then including all modes, substitute Equation (11) into Equation (10) to obtain

$$m \sum_{n=1}^{\infty} z_n \ddot{f}_n + m \sum_{n=1}^{\infty} \bar{\omega}_n^2\ z_n\ f_n = 0 \qquad (12)$$

This is the equation for torsion/chordwise free vibration in a vacuum of the rotating approximate troposkien blade, not including Coriolis coupling with flatwise vibration of the blade.

Reference 2 suggests the following approximate mode shapes for the torsion/chordwise bending vibration of non-rotating circular arcs for the case $\alpha = \pi$ and $y_o = 0$:

$$z_n = R \sin n\theta$$

$$\frac{\beta_n}{\overline{C_n}} = \sin n\theta$$

These expressions were shown in Reference 2 to be approximate solutions to the eigenvalue equation describing the vibration of rotating circular arcs. Note that they satisfy only the pinned-end boundary condition, and are therefore even more approximate for other end conditions, such as the elastic restraint of the curved segment by the straight segments of the approximate troposkien blade.

For the case $\alpha \neq \pi$, the following approximate mode shapes will be used, as for the flatwise modes:

$$z_n = R \sin \left(\frac{n\pi}{\alpha}\right)\theta \tag{13}$$

$$\frac{\beta_n}{\overline{C_n}} = \sin \left(\frac{n\pi}{\alpha}\right)\theta \tag{14}$$

The vibration frequencies are given by the expression

$$\bar{\omega}_n^2 = \bar{\omega}_{n_o}^2 + \bar{K}_n \Omega^2 \tag{15}$$

where $\bar{\omega}_{n_o}$ and $\bar{K}_n$ must be determined experimentally, or numerically by finite-element analysis. For the special case of Reference 2, $\bar{K}_n = n^2-1$.

Then Equations (12), (13), and (14) describe approximately the torsion/chordwise bending free vibration in a vacuum of the circular-arc segment of the rotating approximate troposkien blade.

Note that Equation (9) expresses the structural coupling between torsion and chordwise bending of the circular arc. Substitution of Equations (13) and (14) into Equation (9) yields the nth mode structural coupling coefficient for circular arcs having pinned ends,

$$C_n = \frac{R\beta_n}{z_n} = -\left(\frac{n\pi}{\alpha}\right)^2 \frac{1+k}{1+k\left(\frac{n\pi}{\alpha}\right)^2} \tag{16}$$

This approximate relation was investigated experimentally in Reference 6 and found to be valid for the troposkien blade with pinned ends for the case n = 2, if an effective value $\alpha_{eff} = 2.8$ is used to account for the flexibility of the straight segments of the blade.

For the case of clamped ends, the approximate nth mode structural coupling coefficient for circular arcs with clamped ends is shown in Reference 6 to be

$$C_n = \left[\frac{0.75}{\sin^2\left(\frac{n\pi}{\alpha}\right)\theta} - 2.25\right] \left(\frac{n\pi}{\alpha}\right)^2 \frac{1+k}{1+k\left(\frac{n\pi}{\alpha}\right)^2}$$

where the effective value $\alpha_{eff} = 2.8$ again applies.

Equation (16) is believed to be a reasonable approximation for the structural coupling coefficient of practical blade configurations in the absence of a more precise determination by finite element analysis of the blade.

5. Blade Flutter Equations

Adding the Coriolis forces due to blade bending, and the blade aerodynamic lift force, as shown in Figures 2 and 3, Equations (5) and (12) become

$$\sum_{n=1}^{\infty} m\, y_n\, \ddot{g}_n + \sum_{n=1}^{\infty} m\, \omega_n^2\, y_n\, g_n + \sum_{n=1}^{\infty} 2m\Omega\, z_n\, \dot{f}_n = \frac{1}{R}\frac{dL}{d\theta}\sin\delta \tag{17}$$

$$-\sum_{n=1}^{\infty} 2m\Omega\, y_n\, \dot{g}_n + \sum_{n=1}^{\infty} m\, z_n\, \ddot{f}_n + \sum_{n=1}^{\infty} m\, \bar{\omega}_n^2\, z_n\, f_n = 0 \tag{18}$$

where chordwise aerodynamic forces are neglected.

Using Equations (6) and (13), multiplying Equations (17) and (18) by $R \sin(\frac{n\pi}{\alpha})\theta$, and integrating from 0 to α, the coupled equations of motion in the nth mode are obtained:

$$I_n \ddot{g}_n + I_n \omega_n^2 g_n + 2I_n \Omega \dot{f}_n = \int_0^\alpha \sin\delta \sin(\frac{n\pi}{\alpha})\theta \frac{dL}{d\theta} d\theta \tag{19}$$

$$-2I_n \Omega \dot{g}_n + I_n \ddot{f}_n + I_n \bar{\omega}_n^2 f_n = 0 \tag{20}$$

where $I_n = \int_0^\alpha m R^2 \sin^2(\frac{n\pi}{\alpha})\theta \, d\theta$

and noting that $\int_0^\alpha \sin(\frac{n\pi}{\alpha})\theta \sin(\frac{m\pi}{\alpha})\theta \, d\theta = 0$.

Following Reference 7 and Figure 3, the aerodynamic lift for the wind turbine rotating in <u>still</u> air at constant rotational speed Ω is

$$\frac{1}{R}\frac{dL}{d\theta} = -\frac{1}{8}\rho a c^2 \Omega y_1 \dot{\beta} - \frac{1}{2}\rho a c \Omega y_1 C(k) [\dot{y} \sin\delta + \Omega y_1 \beta + (0.5c - x_A)\dot{\beta}]$$

where ρ = air density

a = blade section lift curve slope

c = blade chord

β = blade twist angle (postive nose down) (see Fig. 2)

y_1 = outer blade undisturbed shape = $y_o + R \sin\delta$

$C(k)$ = Theodorsen's lift deficiency function

x_A = distance from section aerodynamic center to blade elastic axis, positive when A.C. is forward.

Neglecting the $\dot{\beta}$ terms since $c << R$, multiplying by $R \sin(\frac{n\pi}{\alpha})\theta$ and dividing $I_n \Omega^2$, there results

$$\frac{1}{I_n\Omega^2}\int_0^{\pi} \sin\delta \sin(\frac{n\pi}{\alpha})\theta \frac{dL}{d\theta} d\theta = - m_{\dot{g}}\dot{g}_n - m_\beta C_n f_n$$

where $C_n = \frac{R\beta_n}{z_n}$ as before.

Then

$$m_{\dot{g}} = \frac{\gamma}{2}\overline{C(k)} \quad \frac{\int_0^{\alpha}(y_o/R + \sin\delta)\sin^2\delta \sin^2(\frac{n\pi}{\alpha})\theta \, d\theta}{\int_0^{\alpha}\sin^2(\frac{n\pi}{\alpha})\theta \, d\theta}$$

$$m_\beta = \frac{\gamma}{2}\overline{C(k)} \quad \frac{\int_0^{\alpha}(y_o/R + \sin\delta)^2 \sin\delta \sin^2(\frac{n\pi}{\alpha})\theta \, d\theta}{\int_0^{\alpha}\sin^2(\frac{n\pi}{\alpha})\theta \, d\theta}$$

where $\gamma = \frac{\rho acR}{m}$

$\overline{C(k)}$ = typical value of C(k) evaluated at $y_1 = y_o + R\sin\bar{\delta}$ (see Appendix), and the contributions of modes other than the nth are neglected.

Dividing Equations (23) and (24) by $I_n\Omega^2$ and including the aerodynamic terms,

$$\frac{\ddot{g}_n}{\Omega^2} + m_{\dot{g}}\frac{\dot{g}_n}{\Omega} + \nu_n^2 g_n + 2\frac{\dot{f}_n}{\Omega} + m_\beta C_n f_n = 0 \qquad (21)$$

$$-2\frac{\dot{g}_n}{\Omega} + \frac{\ddot{f}_n}{\Omega^2} + \bar{\nu}_n^2 f_n = 0 \qquad (22)$$

where $\nu_n = \frac{\omega_n}{\Omega} = [(\frac{\omega_{n_o}}{\Omega})^2 + K_n]^{1/2}$

$$\bar{\nu}_n = \frac{\bar{\omega}_n}{\Omega} = [(\frac{\bar{\omega}_{n_o}}{\Omega})^2 + \bar{K}_n]^{1/2}$$

These are the flutter equations for the wind turbine rotating in still air.

5. Calculation of Flutter Boundaries

Assume the following solutions to Equations (21) and (22):

$$g_n = \bar{g}_n \, e^{\nu\Omega t} \tag{23}$$

$$f_n = \bar{f}_n \, e^{\nu\Omega t} \tag{24}$$

where $\nu = \frac{\sigma}{\Omega} + i\,\frac{\omega}{\Omega}$. Assume at present that $\overline{C(k)} = 1$.

Substitution of Equations (23) and (24) in Equations (21) and (22) results in two coupled homogeneous algebraic equations. For a solution to exist, the determinant of coefficients must vanish; i.e.,

$$\begin{vmatrix} (\nu^2 + m_{\dot{g}}\nu + \nu_n^2) & (2\nu + m_\beta C_n) \\ -2\nu & [\nu^2 + \bar{\nu}_n^2] \end{vmatrix} = 0$$

Expanding the determinant yields the characteristic equation of the system:

$$A\nu^4 + B\nu^3 + C\nu^2 + D\nu + E = 0$$

where the coefficients are combinations of the system parameters. Then by Routh's criteria for system stability

$$A, B, C, D, E \geq 0 \tag{25}$$

and

$$BCD - AD^2 - B^2E \geq 0 \tag{26}$$

It is now possible to determine the values of $\bar{\nu}_n^2$ required to satisfy conditions (25) and (26) for a given blade configuration. Since

$$\nu_n^2 = \left(\frac{\omega_{n_o}}{\Omega}\right)^2 + K_n$$

and $\bar{\nu}_n^2 = \left(\frac{\bar{\omega}_{n_o}}{\Omega}\right)^2 + \bar{K}_n$

the values of rotational speed at which flutter or divergence will occur (Ω_F) are then specified for given non-rotating flatwise and torsional frequencies ω_{n_o} and $\bar{\omega}_{n_o}$.

In the present case, the characteristic equation is

$$\nu^4 + m_{\dot{g}}\nu^3 + (4 + \nu_n^2 + \bar{\nu}_n^2)\nu^2 + (m_{\dot{g}}\bar{\nu}_n^2 + 2m_\beta C_n)\nu + \nu_n^2 \bar{\nu}_n^2 = 0$$

Then conditions (25) and (26) determine the rotational speed at flutter, Ω_F.

Applying condition (25), flutter occurs when

$$\bar{\nu}_n^2 = -2\frac{m_\beta}{m_{\dot{g}}} C_n \tag{27}$$

Applying condition (26), flutter occurs when

$$\bar{\nu}_n^2 = \frac{2m_\beta^2 C_n^2 - 4m_\beta m_{\dot{g}} C_n - m_\beta m_{\dot{g}} C_n \nu_n^2}{2m_{\dot{g}}^2 - m_\beta m_{\dot{g}} C_n} \tag{28}$$

6. Application to an Existing Blade

The theory developed above is now applied to the preliminary prediction of the flutter of the blades of the Sandia seventeen-meter wind turbine. For this turbine the parameters for the geometry of the circular arc portion of the blade are

$$y_o = 9.10 \text{ ft.}$$

$$R = 18.33 \text{ ft.}$$

$$\alpha = 2 \text{ rad.}$$

For this case it can be shown that $m_\beta \approx 1.575\, m_{\dot{g}}$ Also from Equation (16) for n = 2, k = .0512, $\alpha_{eff} = 2.8$ (Ref. 6):

$$C_n = -4.2$$

Applying Equation (27), flutter occurs when

$$\bar{\nu}_n^2 = 13.2$$

From Reference (8), for the seventeen-meter blade,

$$\bar{\nu}_2^2 = \left(\frac{324}{\Omega_F}\right)^2 + 7.70$$

Equating and solving the two expressions for $\bar{\nu}_2^2$,

$$\Omega_F = 138 \text{ rpm}$$

Applying Equation (28) flutter occurs when

$$\bar{\nu}_2^2 = 13.2 + 0.768\ \nu_2^2$$

From Reference (8), for the seventeen-meter blade,

$$\nu_2^2 = \left(\frac{215}{\Omega_F}\right)^2 + 6.76$$

Then $$\bar{\nu}_2^2 = 18.4 + 0.768\ \left(\frac{215}{\Omega_F}\right)^2$$

Equating and solving the two expressions for $\bar{\nu}_2^2$,

$$\Omega_F = 80.4 \text{ rpm}$$

Here Equation (28) is evidently the critical case.

Final prediction of the flutter speed requires accurate determination of the structural coupling coefficient C_n by finite element analysis.

7. Conclusions

(1) Coriolis forces provide the dominant coupling between flatwise bending and torsion/chordwise bending of the blade. (Also see Reference 2).

(2) Blade flatwise bending velocity and blade torsional displacement contribute the dominant aerodynamic forces acting on the blade.

(3) Accurate determination of the structural coupling between blade torsion and blade chordwise bending is essential to blade flutter prediction.

(4) The following parameters determine the rotational speed at flutter for troposkien-type blades:

(a) blade geometry y_o, R, α (see Figure 1).

(b) blade torsion/chordwise bending structural coupling coefficient C_2 for the second mode.

(c) blade rotating and non-rotating flatwise bending frequencies ω_2 and ω_{2_o} for the second mode.

(d) blade rotating and non-rotating torsion/chordwise bending frequencies $\bar{\omega}_2$ and $\bar{\omega}_{2_o}$ for the second mode.

REFERENCES

1. Blackwell, B.F. and Reis, G.E., "Blade Shape for a Troposkien Type of Vertical-Axis Wind Turbine", Sandia Laboratories Report SAND 74-0154, April 1974.

2. Ham, N.D., "Aeroelastic Analysis of the Troposkien-Type Wind Turbine", Sandia Laboratories Report SAND 77-0026, April 1977.

3. Reis, G.E. and Blackwell, B.F., "Practical Approximations to a Troposkien by Straight-Line and Circular-Arc Segments", Sandia Laboratories Report SAND 74-0100, March 1975.

4. Den Hartog, J.P., "The Lowest Natural Frequency of Circular Arcs", Phil. Mag. 5 (Series 7), 400, 1928.

5. Ojalvo, I.U., "Coupled Twist-Bending Vibrations of Incomplete Elastic Rings", International Journal of Mechanical Sciences, 4, pp. 53-72, 1962.

6. Ham, N.D., "An Investigation of the Structural Coupling Coefficient and Torsional Frequency of Troposkien-Type Wind Turbine Blades with Application to Blade Flutter Prediction", Sandia Laboratories Report in preparation, 1977.

7. Miller, R.H. and Ellis, C.W., "Blade Vibration and Flutter", Journal of the American Helicopter Society, 1, 3, July 1956.

8. Barzda, J., Kaman Aerospace Corp., Bloomfield, Conn., unpublished communication.

DISCUSSION

Comment: I would like to reemphasize the significance of Professor Ham's conclusions that a) quarter-chord mass balancing of the turbine blades is unimportant with regard to flutter speed location, and b) increasing torsional stiffness is an effective method of increasing flutter speed. The impact of the first conclusion on design and fabrication of low cost blades is very favorable, and knowledge of the second conclusion is valuable to the designer. At the same time, I would like to de-emphasize the threat of encountering flutter in any particular blade design. Based on Professor Ham's analysis, blade property evaluation, field experience, and consultation with fabricators, it is relatively easy to design a blade that will not flutter.

Q: Do you agree with R. Reuter that it is relatively easy to design Darrieus blades which do not flutter in their operating regime?

A: Yes.

Q: Am I correct in presuming that the forced response to periodic stalling should also be independent of the chordwise c.g. of the blade sections, and also of the chordwise shear center?

A: Yes.

Q: What were your assumptions relative to the aerodynamics; was the free stream velocity zero? If not what of the resultant periodic coefficient?

A: In the analysis the free stream velocity was assumed to be zero. If this were not so, harmonic airloads would be generated and would cause a forced blade response at various integral multiples of rotor speed. However, in a linear analysis, this forced response is uncoupled with any self-excited motion such as flutter. Experimentally, model blade flutter occurred at the same rotor rotational speed whether or not there was an incident wind.

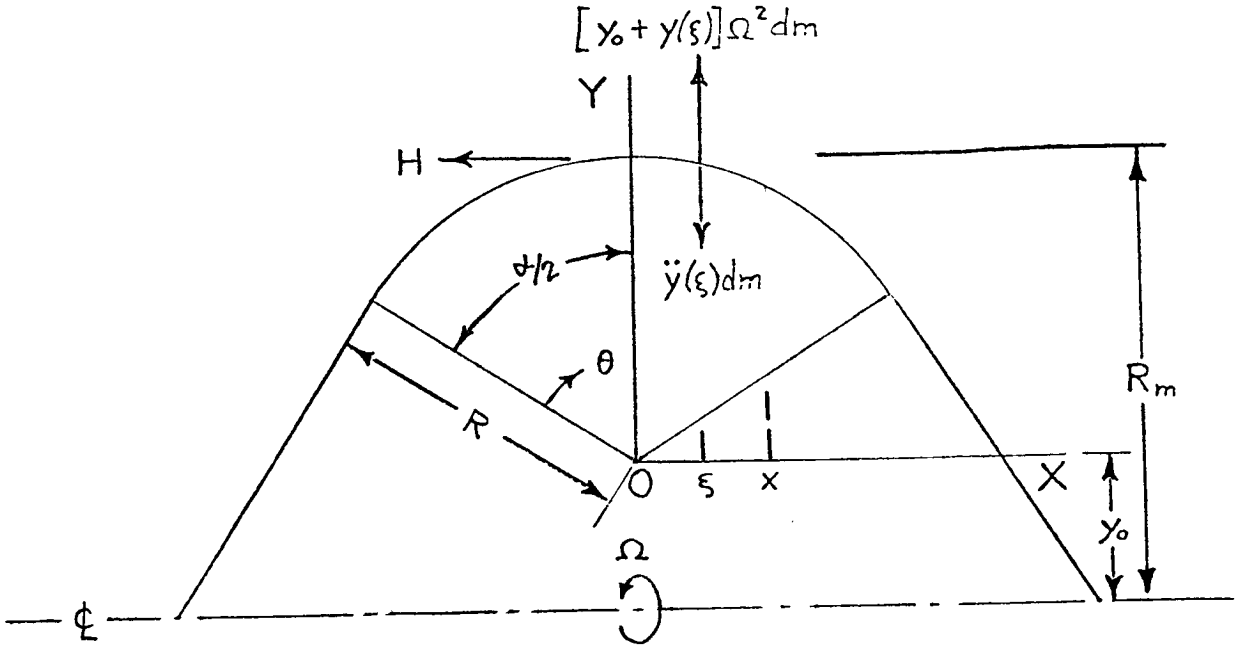

Figure 1. - Blade geometry.

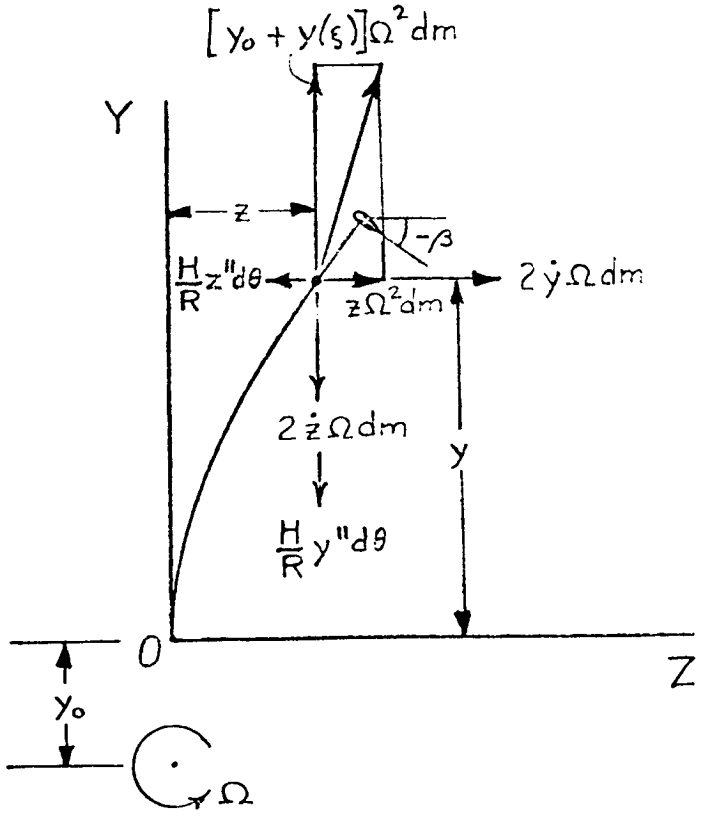

Figure 2. - Blade dynamics.

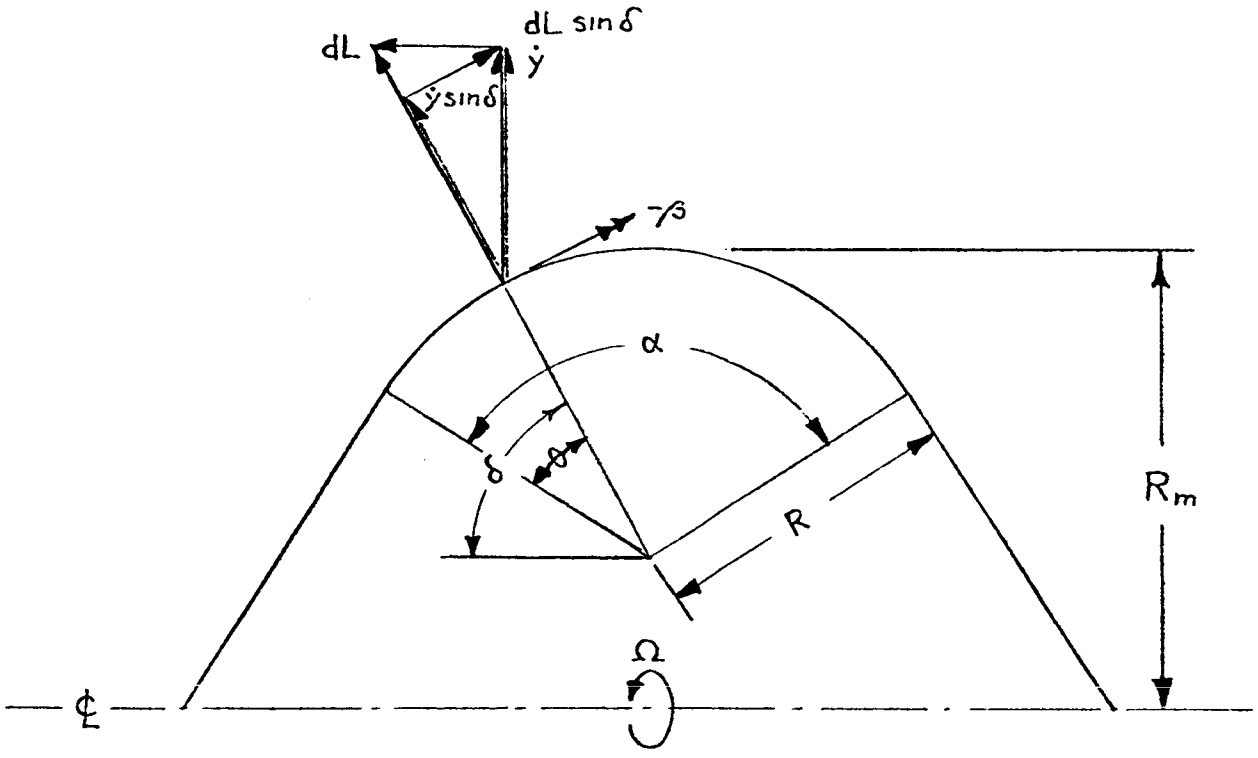

Figure 3. - Blade aerodynamics.